

# The ion environment near Europa and its role in surface energetics

C. Paranicas and B. H. Mauk

Johns Hopkins University Applied Physics Laboratory, Laurel, MD 20723, USA

J. M. Ratliff

Jet Propulsion Laboratory, Pasadena, CA 91109, USA

C. Cohen

California Institute of Technology, Pasadena, CA 91125, USA

R. E. Johnson

University of Virginia, Charlottesville, VA 22903, USA

Received 24 September 2001; revised 8 January 2002; accepted 9 January 2002; published 14 March 2002.

[1] This paper gives the composition, energy spectra, and time variability of energetic ions measured just upstream of Europa. From 100 keV to 100 MeV, ion intensities vary by less than a factor of  $\sim 5$  among Europa passes considered between 1997 and 2000. We use the data to estimate the radiation dose rate into Europa's surface for depths 0.01 mm – 1 m. We find that in a critical fraction of the upper layer on Europa's trailing hemisphere, energetic electrons are the principal agent for radiolysis, and their bremsstrahlung photon products, not included in previous studies, dominate the dose below about 1 m. Because ion bombardment is more uniform across Europa's surface, the radiation dose on the leading hemisphere is dominated by the proton flux. Differences exist between this calculation and published doses based on the E4 wake pass. For instance, proton doses presented here are much greater below 1 mm. *INDEX TERMS*: 6218 Planetology: Solar System Objects: Jovian satellites; 5737 Planetology: Fluid Planets: Magnetospheres (2756); 2720 Magnetospheric Physics: Energetic particles, trapped

## 1. Introduction

[2] Since the discovery by Pioneer and Voyager of a hot plasma trapped in Jupiter's magnetosphere, there has been considerable interest in its effect on the surfaces of the icy Galilean satellites. Although it was suggested that the hemispheric differences in reflectance might be attributed to the plasma bombardment [see, e.g., Johnson *et al.*, 1988], early emphasis was on atmospheric production by sputtering of surface materials [Lanzerotti *et al.*, 1978; Brown *et al.*, 1982]. Recent spectral imaging of the moons by the Galileo spacecraft [McCord *et al.*, 1998] has focused our attention on the role charged particles play in modifying the reflectance properties of these satellites [Carlson *et al.*, 1999]. To quantify this process, estimates of the charged particle bombardment rate have been made using Galileo data [Cooper *et al.*, 2001; Paranicas *et al.*, 2001]. Previous studies of the ions have used measurements taken in Europa's wake (E4) to estimate the radiation dose rate into Europa's surface. Here we use data from very close upstream passes of Europa to describe both the population and time variability of the energetic ions. These data are then used to calculate that radiation dose rate which chemically modifies the surface producing, for instance, the sulfur cycle

[Carlson *et al.*, 1999] and a tenuous oxygen atmosphere [Hall *et al.*, 1998].

[3] Ip *et al.* [1998], Paranicas *et al.* [1999a, 1999b], and Cooper *et al.* [2001] have all presented ion energy spectra based on data from the E4 encounter, which was a wake pass. Since the E4 analysis was done, we have modified our technique for computing the energy spectra of the heavy ions (see section 2). What is also unique to the spectra presented here is that they are all created from upstream data, allow for an estimate of time variability, and, in one case, extend the energy range to several hundred MeV by adding Galileo Heavy Ion Counter (HIC) data to the Energetic Particles Detector (EPD) data.

[4] In this work, we also present the dose rate at depth in ice for different particle species. Measured ion and electron intensities upstream of the satellite and a very simple picture of the satellite as electromagnetically inert, provide an upper limit on the flux of charged particles into Europa's surface. In reality, the electromagnetic picture is more complicated [Kivelson *et al.*, 1999], and the upstream flux, which actually reaches the surface, is a function of particle species, energy, pitch, and phase angle. Since these measurements are made very close to the satellite, the dose rates calculated here are the best possible estimate without explicitly including the local fields and tracking ions to the surface.

## 2. Energy Spectra

[5] In this section we discuss how the data are fit. The encounters considered occurred at a variety of Jovian local times and positions relative to the current sheet: near the center (E12), above it (E19), and well below it (E26). Figure 1 shows total intensity (ions/cm<sup>2</sup>-s-sr-keV) as a function of energy for the dominant ions considered (protons, oxygen, and sulfur). Fits in this figure are not extrapolated, instead they begin at nominal instrument threshold energies for each species. EPD individual and total ion count rates and HIC oxygen intensities were simultaneously fit. A separate fit function for each major species has been used with the functional form

$$j = cE(E + kT(1 + \gamma_1))^{-1-\gamma_1} \times \left(1 + \left(\frac{E}{E_T}\right)^{\gamma_2}\right)^{-1}. \quad (1)$$

Here  $c$ ,  $kT$ ,  $E_T$ ,  $\gamma_1$ , and  $\gamma_2$  are free parameters,  $E$  is the particle energy,  $j$  is the intensity. We have found that helium is an important minor constituent ( $\sim 10\%$  of the smaller of oxygen or sulfur intensity), and Maclennan *et al.* [2001] suggest that sodium too is

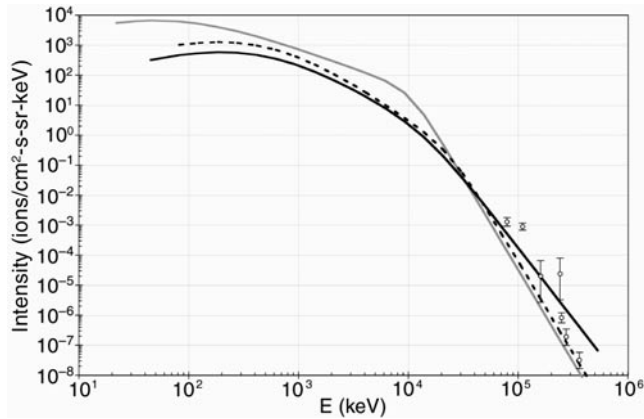


**Figure 1.** Energy spectrum fit to data taken during the E12 encounter. Individual curves show protons (gray solid line), oxygen (black solid line), and sulfur (dashed). HIC data from the E12 encounter are included (circles) with error bars.

routinely detected at low intensities, but this ion was not included in our fits. The EPD data used here are from the E12 encounter on day 350 of 1997 from 1216–1221 UT (hereafter, 1997–350 1216–1221 UT). The EPD data have been corrected for penetrating particles and instrument degradation over the mission lifetime. As in earlier work, penetrating particles were subtracted from the raw counts by using rates in sectors that are shielded. In addition, we have discovered from the pulse-height analysis matrix that individual ion channel counts have been degraded over the mission lifetime. Finally, we have set  $kT_{\text{ox}} = kT_{\text{su}}$ , based on empirical studies of the channels. We omit the details for brevity,

but note that these corrections were not included in the E4 analysis presented by *Ip et al.* [1998] and *Cooper et al.* [2001]; these changes may account, for instance, for the much higher intensities in energetic oxygen reported here.

[6] The HIC data obtained during this time period are somewhat limited statistically but oxygen intensities from several energy intervals were obtained. These intensities were calculated using the raw event data (rather than the rate data), which allows various requirements to be imposed in order to reduce background contributions. The resulting oxygen and sulfur fits given here are in good agreement with a similar fit to the E12 data given by *MacLennan et al.* [2001]. Individual points and error bars for EPD are not displayed because total ion count rates are routinely fit using a sum of individual ion contributions [see *Paranicas et al.*, 1999b for details].

[7] In the same vein as in Figure 1, we fit Europa EPD data from other encounters. The results are presented in Figure 2. Fits are presented for four time periods: E12 (repeated from Figure 1), E19 (1999-032 0201–0205 UT and 0225–0228 UT), and E26 (2000-003 1745–1750 UT). Error bars are drawn on the 1999-032 0201–0205 UT fit only. Here the error bars were created by varying the initial conditions of the fits and the efficiency uncertainties of some low-energy total ion channels. This was done to illustrate the variability of the fit procedure. For instance, the large error bars at low energy in the middle and right-hand panels indicate the lack of individual heavy ion coverage at low energies. Also, to compare intensities across species, we extrapolated the heavy ion fits down to 20 keV, accounting for the large differences among fits below  $\sim 100$  keV. We note, for instance, that the energetic oxygen fits are all in good agreement with the fit including HIC data.

[8] Where we have good coverage of individual species, at lower energies for protons, and higher energies for oxygen and

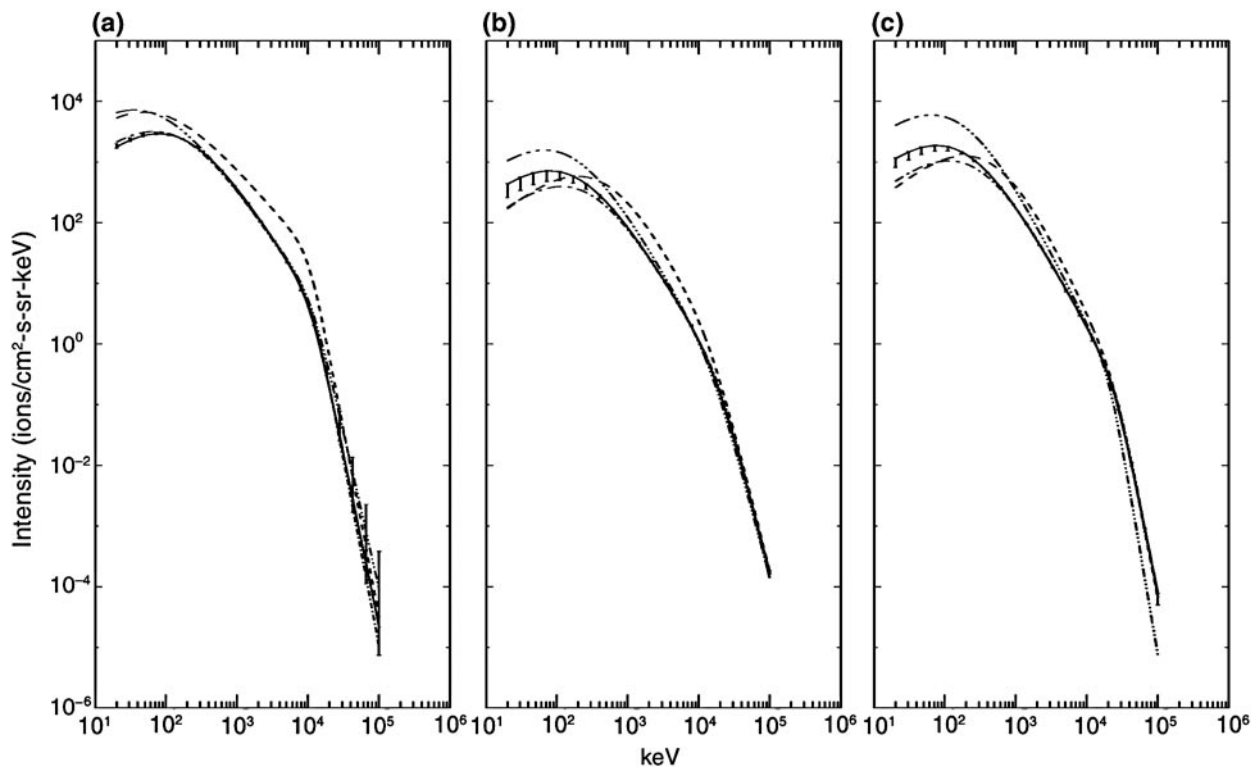


**Figure 2.** Intensity (in ions/cm<sup>2</sup>-s-sr-keV) versus energy for several Europa encounters: E12 (dashed), E19-0201 (solid), E19-0224 (dash-dot), E26 (dash-dot-dot-dot). Panels are (a) protons, (b) oxygen, and (c) sulfur. Uncertainty is represented by error bars on the E19-0201 curves. Data coverage begins at tens of keV and extends to above 100 MeV.

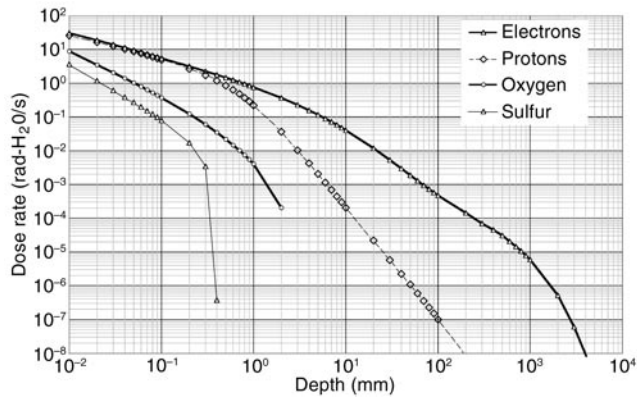


**Figure 3.** Dose rate (rad-H<sub>2</sub>O/sec) versus depth curves for, in order of decreasing dose, electrons, protons, oxygen, and sulfur based on E12 spectra given in Figure 1 and electrons from *Paranicas et al.* [2001].

sulfur, the fits from the different time periods fall near one another. This is surprising because the source of heavy ions at Io's exosphere is variable, the transport mechanism of the ions is influenced by magnetospheric activity, the measurements are made at different local times and locations relative to the current sheet, and the count rates have been corrected to varying degrees over the mission.

### 3. Dose Rate Into Surface

[9] In this section we discuss the radiation dose rate into water ice, based on the fits to the ion data presented in the previous section. If we assume these distributions in the near upstream region are also present on magnetic field lines connected to Europa, then it is straightforward to calculate the rate of energy deposition at the surface:

$$P = \pi \int j(E) E dE. \quad (2)$$

A similar formula was used in *Paranicas et al.* [2001] for electrons. Unlike the energetic electrons, the keV ion fluxes to the trailing hemisphere are only a few times larger than that to the leading [*Pospieszalska and Johnson, 1989*]. For the more energetic ions considered here, which cause radiation effects at depth, the flux difference is much smaller. Therefore, we assume to first order that the energetic ions deposit energy nearly uniformly over the surface.

[10] From the ion fits given above, we find the average power per unit area (in W/m<sup>2</sup>) at the surface, integrated between 10 keV–10 MeV total energy, is,  $P_p = 0.012 (\pm 0.0076)$ ,  $P_{ox} = 0.0025 (\pm 0.0012)$ , and  $P_{su} = 0.0048 (\pm 0.0017)$ . For comparison, we found  $P = 0.057$  W/m<sup>2</sup> for electrons in the same energy range [see *Paranicas et al., 2001*]. Figure 2 of that 2001 paper correctly gives this value as the maximum electron rate even though we accidentally omitted the “2 $\pi$ ” in the corresponding equation. These ion rates would be 15–20% larger if we extended the energy range to 100 MeV. We emphasize that if the entire upstream ion population in the energy range of interest here does reach Europa's surface, it deposits less energy per unit time than the electrons.

[11] The charge state of the incident O and S ions will affect how and where their energy will be deposited in the material, and into which molecule the ion becomes incorporated as it comes to rest. The effect of the charge state is expected to be most pronounced for ions having a total kinetic energy comparable to the energy needed to fully ionize the ion. For O and S this is on the

order of a few keV. An ion with this kinetic energy will stop within the first micron of the ice material.

[12] In addition to estimating the ion power reaching the surface, it makes sense to consider further how the energy is deposited at depth. Figure 3 shows the computed dose in a water ice surface with dose rate given in rads/s (1 rad = 100 erg/gm). The computation includes only the ionizing dose, or energy transferred to the ice via ionization of its constituent atoms. Ionization will be the dominant mechanism for energy transfer at penetration depths considered here (larger than 10 microns). An adjoint Monte Carlo radiation transport computer code was used for the dose computation (T. Jordan, Novice radiation transport software, version update in 2000). The inflection in the uppermost curve near 100 mm indicates the depth at which the bremsstrahlung photons begin to be dominant.

[13] The electron dose rates in Figure 3 are somewhat smaller than, but within a factor of 3 of, our previous estimate [*Paranicas et al., 1999a*] based on the model of *Divine and Garrett* [1983]; the proton curves in the two calculations are almost identical. In our earlier presentation, we also calculated dose vs. depth for a fit to the E4 data in which we extrapolated the proton spectrum far above the EPD range to tens of GeV energies, based on our estimate of the proton spectrum in the heliosphere at 5 AU. The reason for doing that was a lack of new data on 100 MeV to 100 GeV proton intensities. The major difference between Figure 3 and that result is the previous proton doses were more than an order of magnitude larger below 10 mm and dominated the dose below about 1 m.

[14] *Cooper et al.* [2001] have also published an estimate of the radiation accumulation time for a fit to the E4 data at smaller depths. Converting their numbers to rads/s in the range of depth overlap reveals the following. Electron doses are almost identical down to the range they report. Our proton doses are larger by about an order of magnitude at 1 mm and about 2 orders of magnitude at 10 mm. Our calculation for the E19-0201 protons (not shown) are also smaller than the one presented in Figure 3, with the E19 proton doses a factor of 4 smaller at 1 mm and a factor of 2 smaller at 10 mm. A chief reason for the discrepancies among all these calculations is the energy spectrum used. For example, comparing the E12 spectrum presented here to the E4 one [*Cooper et al., 2001*], E12 proton intensities are greater above 10 MeV. These protons have mean ranges beginning at about 1 mm. Differences in the fit procedures, the use of wake vs. upstream data, the time variability effects on the spectra, and different models for calculating the dose at depth all contribute to the range in values.

### 4. Discussion

[15] In this work, we have assumed that ions precipitate uniformly over Europa's surface. This is because an EPD ion's bounce time should well exceed the time its guiding center magnetic field spends in the vicinity of Europa. This would create a situation in which trapped ions precipitate onto Europa's surface in a continuous way, coming from high magnetic latitudes. We can estimate the sputtering rate over the whole surface using the E12 fit and an up-to-date yield function for incident oxygen and sulfur ions on water ice ([www.people.virginia.edu/~rej](http://www.people.virginia.edu/~rej)). Integrating over the energy range, 10<sup>3</sup>–10<sup>6</sup> eV/amu, we find that  $\sim 3 \times 10^{24}$  water molecules/s are liberated by the action of protons,  $\sim 4 \times 10^{26}$  from oxygen ions, and  $\sim 2 \times 10^{27}$  from sulfur ions. This ignores the enhancements due to surface temperature and the decomposition by the electrons and ions that leads to the release of H<sub>2</sub> and O<sub>2</sub>.

[16] The results here confirm that when upstream fluxes of ions and electrons have access to the surface, electrons are a principal chemical agent for the range of depths discussed here, i.e., 0.01 mm – 1 m. Our calculations also show that below about 1 m, bremsstrahlung photons dominate the dose. In a recent paper, we suggested that as flux tubes carry plasma past Europa, they lose the vast majority of energetic electrons to the trailing hemisphere. Energetic ions, on the other hand, produce a much

more uniform dose to the satellite's whole surface. A consequence is that radiolysis of the leading hemisphere of Europa will be dominated by the ion dose rate given in Figure 3. Therefore, we predict a smaller total dose of radiation at various depths on the leading hemisphere than on the trailing one. Since exogenous processes play a role in the observed global differences between the leading and trailing hemispheres, the chemistry with these differential radiation agents and doses now needs to be determined.

[17] **Acknowledgments.** The research presented here was carried out under contracts between NASA and the various member institutions.

## References

- Brown, W. L., L. J. Lanzerotti, and R. E. Johnson, Fast ion bombardment of ices and its astrophysical implications, *Science*, 218, 525, 1982.
- Carlson, R. W., R. E. Johnson, and M. S. Anderson, Sulfuric acid on Europa and the radiolytic sulfur cycle, *Science*, 286, 97, 1999.
- Cooper, J. F., R. E. Johnson, B. H. Mauk, H. B. Garrett, and N. Gehrels, Energetic electron and ion irradiation of the icy Galilean satellites, *Icarus*, 149, 133, 2001.
- Divine, N., and H. B. Garrett, Charged particle distributions in Jupiter's magnetosphere, *J. Geophys. Res.*, 88, 6889, 1983.
- Hall, D. T., P. D. Feldman, M. A. McGrath, and D. F. Strobel, The far-ultraviolet oxygen airglow of Europa and Ganymede, *Astrophys. J.*, 499, 475, 1998.
- Ip, W. H., D. J. Williams, R. E. McEntire, and B. H. Mauk, Ion sputtering and surface erosion at Europa, *Geophys. Res. Lett.*, 25, 829, 1998.
- Johnson, R. E., M. Nelson, T. McCord, and J. Gradie, Voyager images of Europa: Plasma bombardment, *Icarus*, 75, 423–436, 1988.
- Kivelson, M. G., K. K. Khurana, D. L. Stevenson, L. Bennett, S. Joy, C. T. Russell, R. J. Walker, C. Zimmer, and C. Polanskey, Europa and Callisto: Induced or intrinsic fields in a periodically varying plasma environment, *J. Geophys. Res.*, 104, 4609, 1999.
- Lanzerotti, L. J., W. L. Brown, J. M. Poate, and W. M. Augustyniak, On the contribution of water products from Galilean satellites to the Jovian magnetosphere, *Geophys. Res. Lett.*, 5, 155, 1978.
- MacLennan, C. G., L. J. Lanzerotti, and A. Lagg, Hot plasma heavy ion abundance in the inner Jovian magnetosphere (<10 R<sub>J</sub>), *Planet. Space Sci.*, 49, 275, 2001.
- McCord, T. B., et al., Salts on Europa's surface detected by Galileo's Near Infrared Mapping Spectrometer, *Science*, 280, 1242, 1998.
- Paranicas, C., A. F. Cheng, D. J. Williams, K. K. Khurana, M. G. Kivelson, N. Krupp, and A. Lagg, Ion precipitation maps of Europa, AGU abstract, Magnetospheres of the Outer Planets Meeting, Paris, France, 1999a.
- Paranicas, C., W. R. Paterson, A. F. Cheng, B. H. Mauk, R. W. McEntire, L. A. Frank, and D. J. Williams, Energetic particle observations near Ganymede, *J. Geophys. Res.*, 104, 17,459, 1999b.
- Paranicas, C., R. W. Carlson, and R. E. Johnson, Electron bombardment of Europa, *Geophys. Res. Lett.*, 28, 673, 2001.
- Pospieszalska, M. K., and R. E. Johnson, Magnetospheric ion bombardment profiles of satellites: Europa and Dione, *Icarus*, 78, 1, 1989.

---

C. Paranicas, The Johns Hopkins University Applied Physics Laboratory, 11100 Johns Hopkins Road, Laurel, MD 20723-6099. (chris.paranicas@jhuapl.edu)

J. M. Ratliff, Jet Propulsion Laboratory, 4800 Oak Grove Dr., Pasadena, CA 91109.

B. H. Mauk, The Johns Hopkins University Applied Physics Laboratory, 11100 Johns Hopkins Road, Laurel, MD 20723-6099. (barry.mauk@jhuapl.edu)

C. Cohen, California Institute of Technology, Pasadena, CA 91125.  
R. E. Johnson, University of Virginia, Charlottesville, VA 22903.